



Published in final edited form as:

Proc SPIE Int Soc Opt Eng. 2017 March ; 10135: . doi:10.1117/12.2255952.

Deformable 3D-2D Registration for Guiding K-Wire Placement in Pelvic Trauma Surgery

J. Goerres^a, M. Jacobson^a, A. Uneri^a, T. De Silva^a, M. Ketcha^a, S. Reungamornrat^a, S. Vogt^b, G. Kleinszig^b, J.-P. Wolinsky^c, G. Osgood^d, and J.H. Siewerdsen^{a,c,*}

^aJohns Hopkins University, Biomedical Engineering, Baltimore, United States

^bSiemens, Healthcare XP, Erlangen, Germany

^cThe Johns Hopkins Hospital, Department of Neurosurgery, Baltimore, United States

^dThe Johns Hopkins Hospital, Department of Orthopaedic Surgery, Baltimore, United States

Abstract

Pelvic Kirschner wire (K-wire) insertion is a challenging surgical task requiring interpretation of complex 3D anatomical shape from 2D projections (fluoroscopy) and delivery of device trajectories within fairly narrow bone corridors in proximity to adjacent nerves and vessels. Over long trajectories (~10–25 cm), K-wires tend to curve (deform), making conventional rigid navigation inaccurate at the tip location. A system is presented that provides accurate 3D localization and guidance of rigid or deformable surgical devices (“components” – e.g., K-wires) based on 3D-2D registration. The patient is registered to a preoperative CT image by virtually projecting digitally reconstructed radiographs (DRRs) and matching to two or more intraoperative x-ray projections. The K-wire is localized using an analogous procedure matching DRRs of a deformably parametrized model for the device component (deformable known-component registration, or dKC-Reg). A cadaver study was performed in which a K-wire trajectory was delivered in the pelvis. The system demonstrated target registration error (TRE) of 2.1 ± 0.3 mm in location of the K-wire tip (median \pm interquartile range, IQR) and $0.8 \pm 1.4^\circ$ in orientation at the tip (median \pm IQR), providing functionality analogous to surgical tracking/navigation using imaging systems already in the surgical arsenal without reliance on a surgical tracker. The method offers quantitative 3D guidance using images (e.g., inlet/outlet views) already acquired in the standard of care, potentially extending the advantages of navigation to broader utilization in trauma surgery to improve surgical precision and safety.

Keywords

3D/2D registration; deformable registration; trauma surgery; image guidance; surgical navigation

* jeff.siewerdsen@jhu.edu; phone +1 (443) 287-6269; fax +1 (410) 955-9826; www.istar.jhu.edu.

1. DESCRIPTION OF PURPOSE

Percutaneous pelvic fixation is a surgical procedure employed to stabilize a pathological bone condition or restore bone morphology. Surgical screws are inserted along narrow trajectories inside the bone. Since the trajectories can be long (15–25 cm) and are usually accessible via fairly constrained minimally-invasive entry points, Kirschner wires (K-wires) are first inserted to guide cannulated screws along the desired trajectory. Mobile fluoroscopic C-arms are a common system in support of such procedures. The C-arm gantry is typically rotated about the patient to acquire one or more 2D x-ray projection images from various perspectives to provide the surgeon with a (qualitative) 3D reckoning of the location of the implant or tool with respect to the bone shape. This process often requires a high degree of surgical experience and extended fluoroscopy times, e.g., upwards of 123 ± 12 seconds per screw as reported by Gras et al. [1] for pelvic trajectories.

Several methods have been proposed to provide surgical guidance. Optical trackers can be used for percutaneous pelvic navigation [2] using markers fixed to the patient such that they are visible in the pre-operative CT. The marker positioning requires additional surgery preparation and introduces the risk of dislocating the marker from the measured position. Navigation systems with cone-beam CT (CBCT) registered to the optical tracker begin to address this problem and allow accurate tracking with respect to intra-operative image data. However, due to the rigid assumption of optical markers, wire deformation can lead to inaccurate tip localization. Electromagnetic tracking systems can overcome this problem but can experience a loss of accuracy in wire deformation can lead to inaccurate tip localization. Electromagnetic tracking systems can overcome this problem but can experience a loss of accuracy in proximity to metal structures and may require tool-specific manufacturing to accomplish tracking of devices within the body. In contrast to such navigation systems, the C-arm imaging system itself can be used to localize tools using 3D-2D registration, as previously shown in the context of spinal surgery [3],[4]. Based on this approach, we present a new system for accurate K-wire localization from three pelvic inlet- and outlet- view x-ray projections. This approach can help to reduce radiation dose in pelvic surgeries, provide functionality analogous to surgical navigation, and improve patient safety due to accurate localization of the wire with respect to surrounding bone structures.

2. METHODS

2.1 Patient registration

Rigid 3D-2D registration is a common approach to determine 3D information based on 2D x-ray projections. A known object, e.g. in a CT image, is rigidly transformed according to its virtual projections (DRRs) to optimally match the real x-ray projections. This technique is applied to determine the patient transform T_p that transfers the CT volume to the patient location inside the intraoperative C-arm orbit. The CT is virtually projected by computing DRRs for each view θ . Virtual rays $\vec{r}(T_\theta)$ are projected through the CT volume with respect to rigid extrinsic parameters T_θ of projective geometry and integrated using linear interpolation to obtain $DRR(V, T_p) = \int_{\vec{r}} V(T_p) d\vec{r}(T_\theta)$. The optimization leading to

transform T_p is based on the similarity between the projection and the DRR represented by the pixel-wise gradient correlation (GC):

$$GC(f, m) = \frac{1}{2} \left\{ \frac{\nabla_x f \nabla_x m}{\|\nabla_x f\| \|\nabla_x m\|} + \frac{\nabla_y f \nabla_y m}{\|\nabla_y f\| \|\nabla_y m\|} \right\} \quad (1)$$

and ∇ is the gradient operator applied to the fixed radiograph (f) and moving DRR (m) images. The optimization function computes the CT volume transform that maximizes the GC similarity between projections P_θ and the DRR:

$$T_p = \arg \max_T GC \sum_\theta (P_\theta, \int_{\vec{r}} V(T) d\vec{r}(T_\theta)) \quad (2)$$

For optimization, the evolutionary algorithm CMA-ES [5] was applied using 400 populations and an initial variance of $\sigma = 10$. The transform T is represented by a 6-dimensional parameter vector consisting of position and Euler angles.

2.2 Deformable known-component registration (dKC-Reg)

To localize the wire, a registration is computed in which, instead of the CT volume V , a parametrizable mesh object $C(p)$, e.g. a cylinder of variable length and size, is resized and transformed until its DRRs optimally match the x-ray projections:

$$\hat{p} = \arg \max_p \sum_\theta GC(P_\theta, \int_{\vec{r}} C(p) d\vec{r}(T_\theta)) \quad (3)$$

Since K-wires are prone to deformation and a rigid cylinder likely converges at the longest line segment, e.g. at irrelevant location outside the patient, we apply a deformable cylinder component $C(p)$ as presented by Uneri et al. [4]. The parameter vector p of this component describes shape, transform, and size. It incorporates a B-spline deformation:

$$C(u) = \sum_{i=0}^n \alpha_i N_{i,k}(u) \quad (4)$$

where control points $\alpha_i \in p$ are a subset of the parameter vector \hat{p} and $N_{i,k}$ are the B-Spline basis functions. To ensure that the curve legs are tangent to the first and last control point, the spline is clamped by constraining the first and last knots to $u_0 = u_1 \dots = u_k$ and $u_{n+1-k} = \dots = u_n = u_{n+1}$. The cylindrical mesh (Figure 1a) is constructed about the centerline by sampling positions d_j along the spline where perpendicular discs of radius $r \in p$ are created for mesh tessellation. We modeled the K-wire as a cubic spline ($k = 3$) of order $n = 3$ and initialized with 200 mm length and 1.6 mm radius.

2.3 C-Arm setup and calibration

A motorized mobile C-arm (Cios Alpha, Siemens Healthineers, Erlangen, Germany) was used as the imaging system in this work. The C-arm was oriented in line with the operating table to allow truth definition of K-wire placement via cone-beam (CBCT) reconstruction in this study. At each K-wire position delivered to the cadaver, 78 projections (126 kV, 91 mA) were acquired ranging from -37.6° to 15.9° about the LR axis - i.e., a range of typical “inlet” and “outlet” views that are commonly acquired in pelvic trauma fluoroscopy. Three of these projections (-37.6° , -10.2° , 15.9°) were used for the actual K-wire localization, and the remaining views were used to determine the true wire location. An additional 445 angular projections (about the SI axis) covering 300° were acquired to reconstruct the CBCT scan, in which the tip segment of the K-Wire was manually annotated. To determine C-arm projection geometries T_θ for each view θ , an automatic view calibration [6] was performed, which used a cylindrical phantom with well-defined arrangements of radiopaque sphere locations for single-view projection geometry estimation. Since the calibration phantom was designed for planar scan trajectories, the angular and orbital scan arcs had to be calibrated separately with the phantom in two different positions. The two calibrations were later aligned to a common 3D coordinate system by 3D-2D registration of a CBCT volume - reconstructed from the angular acquisition - to the 75 orbital projections. The three views used for K-wire localization were removed in this process to avoid a registration bias towards the solution.

2.4 Cadaver experiment

The dKC-Reg system was evaluated in a study involving a human cadaver in which a variety of pelvic K-wires were delivered. The cadaver was first scanned using a multidetector CT (MDCT) scanner with fairly standard technique protocol appropriate to preoperative planning (120 kVp, 500 mAs, $0.35 \times 0.35 \times 0.80 \text{ mm}^3$ voxels; Philips Brilliance 64- slice MDCT). With the cadaver placed in supine position, a K-wire was inserted into the left hip following a standard pelvic trajectory from the iliac crest to the posterior column. At three milestone positions along the trajectory, the orbital projection views (inlet/outlet) as well as the angular projections (for CBCT truth definition) were acquired. These trajectory positions are also visualized in Figures 2a–2c. The wires were inserted by a fellowship-trained surgeon using Stryker K-wires of 3.2 mm diameter with threaded tip. Registration accuracy was evaluated at the tip location by

$$\text{TRE}_x = \|C(\alpha_0) - C_{\text{true}}(\alpha_0)\|_2, \quad \text{TRE}_\phi = \cos^{-1} \frac{c'(\alpha_0) \cdot c'_{\text{true}}(\alpha_0)}{\|c'(\alpha_0) \cdot c'_{\text{true}}(\alpha_0)\|} \quad (5)$$

where α_0 is the spline control point for the K-wire tip. The patient transform T_p was manually initialized, displaced by $40.5 \pm 31.8 \text{ mm}/25.3 \pm 22.6^\circ$ (median \pm interquartile range, IQR) and the cylinder component was initialized based on a manually annotated plan in the preoperative CT image, displaced by $78.1 \pm 44.3 \text{ mm}/6.4 \pm 3.3^\circ$ (median \pm IQR).

3. RESULTS

The results for TRE_x and TRE_ϕ are shown in Figures 3a and 3b for each trajectory position a–c over 10 restarts to demonstrate a robust converging behavior of the evolutionary optimization. Pooling the trajectory results lead to $TRE_x = 2.1 \pm 0.3$ mm and $TRE_\phi = 0.8 \pm 1.4^\circ$ (median \pm IQR). In order to investigate the advantage over a rigid tracking system, we measured wire deformations based on the distance between tip and a line defined at cortex entry, obtaining the value 8.2 mm (at position c). Moreover, using a deformable instead of a rigid component improved the TRE_x by 39.9 ± 111.5 mm (median \pm IQR) due to 40% failure (diverging to local maxima far from the solution) in the rigid approach. The difference in TRE_ϕ between rigid and deformable remained similar with $-0.2^\circ \pm 5.7^\circ$ (median \pm IQR). In Figure 1b, a maximum intensity projection of the pre-operative CT is shown with a color-coded overlay of the deformed components. Figure 1c shows the known-component overlaid on the x-ray projection, demonstrating an accurate fit to the deformed wire. Figure 4 shows all involved image representations in the registration at trajectory position c. Shown are the three projections, the DRRs for corresponding geometry, and a map of the GC similarity metric.

5. CONCLUSIONS

We have presented a novel deformable K-wire localization and guidance method for mobile C-arm systems based on three calibrated projections of standard pelvic views. Due to the consecutive 3D-2D registrations of the patient and component, the K-wire can be overlaid on the preoperative CT for guidance analogous to conventional surgical navigation (but without external tracking systems) updated at each milestone inlet/outlet view. In this way, the registration approach provides 3D guidance using two or three radiographic views already acquired within the standard of care for fluoroscopically guided procedures. Accurate registration was demonstrated by a median localization error smaller than the K-wire thickness. The current implementation treats the pelvis as a single rigid body, which is appropriate to simple fractures. Future work will extend the framework to multiple rigid bodies - e.g., complex fracture. The framework is capable of handling multiple device components and could offer an improvement in surgical precision and safety in trauma surgery.

Acknowledgments

This research was supported by NIH grant R01-EB-017226 and academic industry partnership with Siemens Healthineers (XP Division, Erlangen, Germany). Sincere thanks Dr. Wojciech Zbijewski (Biomedical Engineering, Johns Hopkins University) for valuable discussion and assistance with the cadaver study.

References

1. Gras F, Marintschev I, Wilharm A, Klos K, Mückley T, Hofmann GO. 2D-fluoroscopic navigated percutaneous screw fixation of pelvic ring injuries. *BMC Musculoskeletal Disorders*. 2010; 11:153. [PubMed: 20609243]
2. Barrick EF, O'mara JW, Lane HE. Iliosacral Screw Insertion Using Computer-Assisted CT Image Guidance: a Laboratory Study. *Computer Aided Surgery*. 1998; 3(6):289–296. [PubMed: 10379978]

3. Uneri A, Silva TD, Stayman JW, Kleinszig G, Vogt S, Khanna AJ, Gokaslan ZL, Wolinsky JP, Siewerdsen JH. Known-component 3D–2D registration for quality assurance of spine surgery pedicle screw placement. *Physics in Medicine & Biology*. 2015; 60(20):8007.
4. Uneri A, Goerres J, Silva TD, Jacobson MW, Ketcha MD, Reaungamornrat S, Kleinszig G, Vogt S, Khanna AJ, Wolinsky JP, Siewerdsen JH. Deformable 3D–2D Registration of Known Components for Image Guidance in Spine Surgery. *Medical Image Computing and Computer-Assisted Intervention – MICCAI 2016*. 2016:124–132.
5. Hansen N, Müller SD, Koumoutsakos P. Reducing the Time Complexity of the Derandomized Evolution Strategy with Covariance Matrix Adaptation (CMA-ES). *Evolutionary Computation*. 2003; 11(1):1–18. [PubMed: 12804094]
6. Daly MJ, Siewerdsen JH, Cho YB, Jaffray DA, Irish JC. Geometric calibration of a mobile C-arm for intraoperative cone-beam CT. *Medical Physics*. 2008; 35(5):2124–2136. [PubMed: 18561688]

Author Manuscript

Author Manuscript

Author Manuscript

Author Manuscript

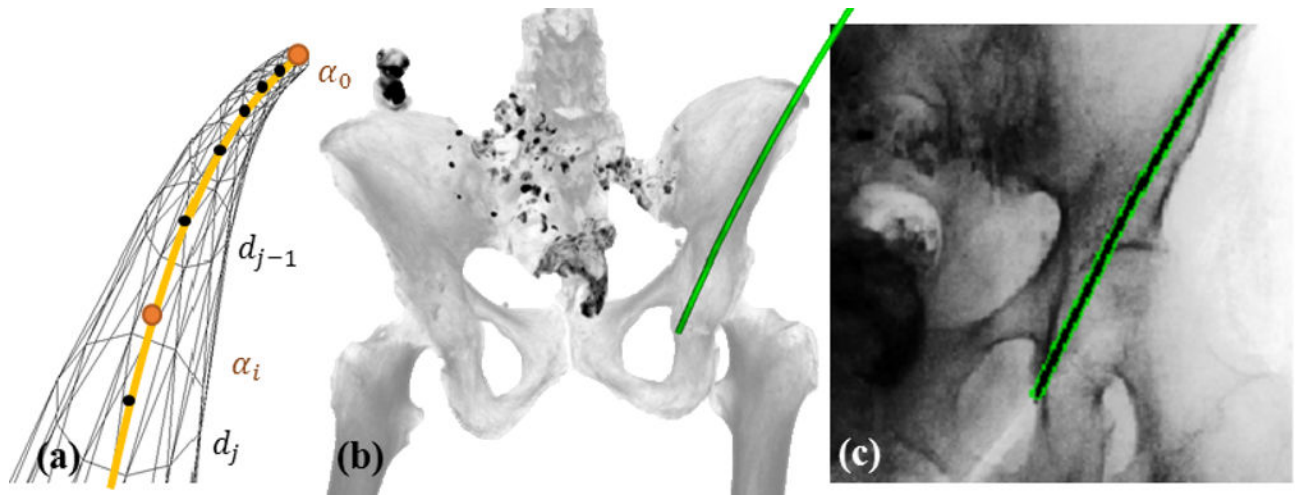


Figure 1. (a) B-spline control points and disc-based mesh tessellation. (b) Maximum intensity projection of the pre-operative CT with registered components for trajectory position c. (c) Projection of deformable known-component overlaid on radiograph.

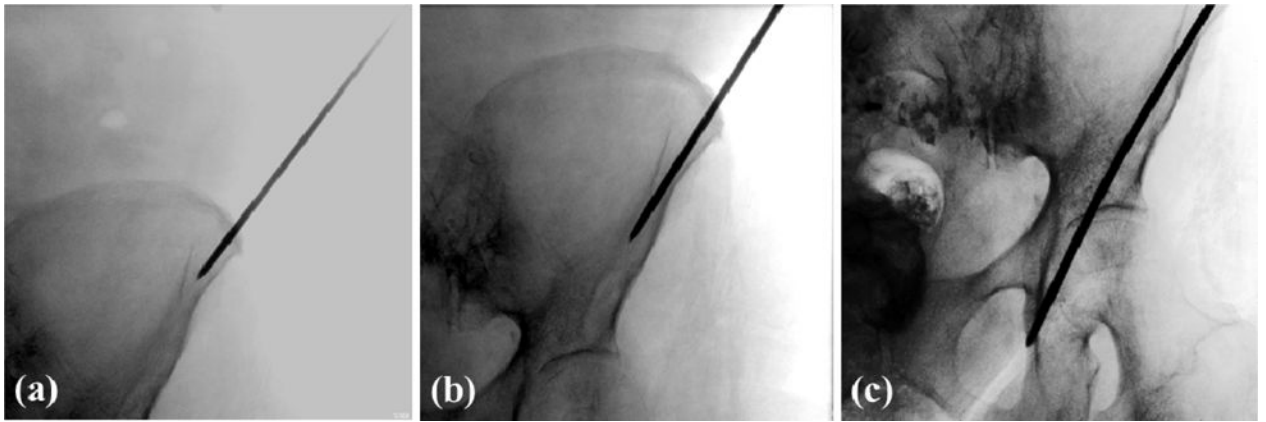


Figure 2. Fluoroscopic images of the wire trajectory being placed from iliac crest to posterior column in the cadaver experiment. Figures (a–c) show the projections at 16° of wire insertion at (a) the time right after insertion, (b) half of the trajectory, (c) final location.

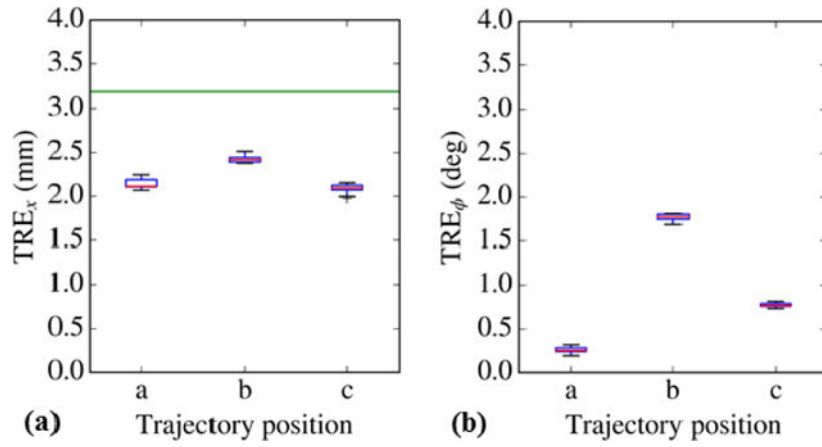


Figure 3. Accuracy of registration at the K-wire tip with respect to (a) distance and (b) angle. The green line in (a) marks the K-wire diameter as a point of comparison. The fairly narrow statistical distribution for each measurement is the result of slight stochastic effects in the optimizer, demonstrating robust behavior despite randomness in the evolutionary process.

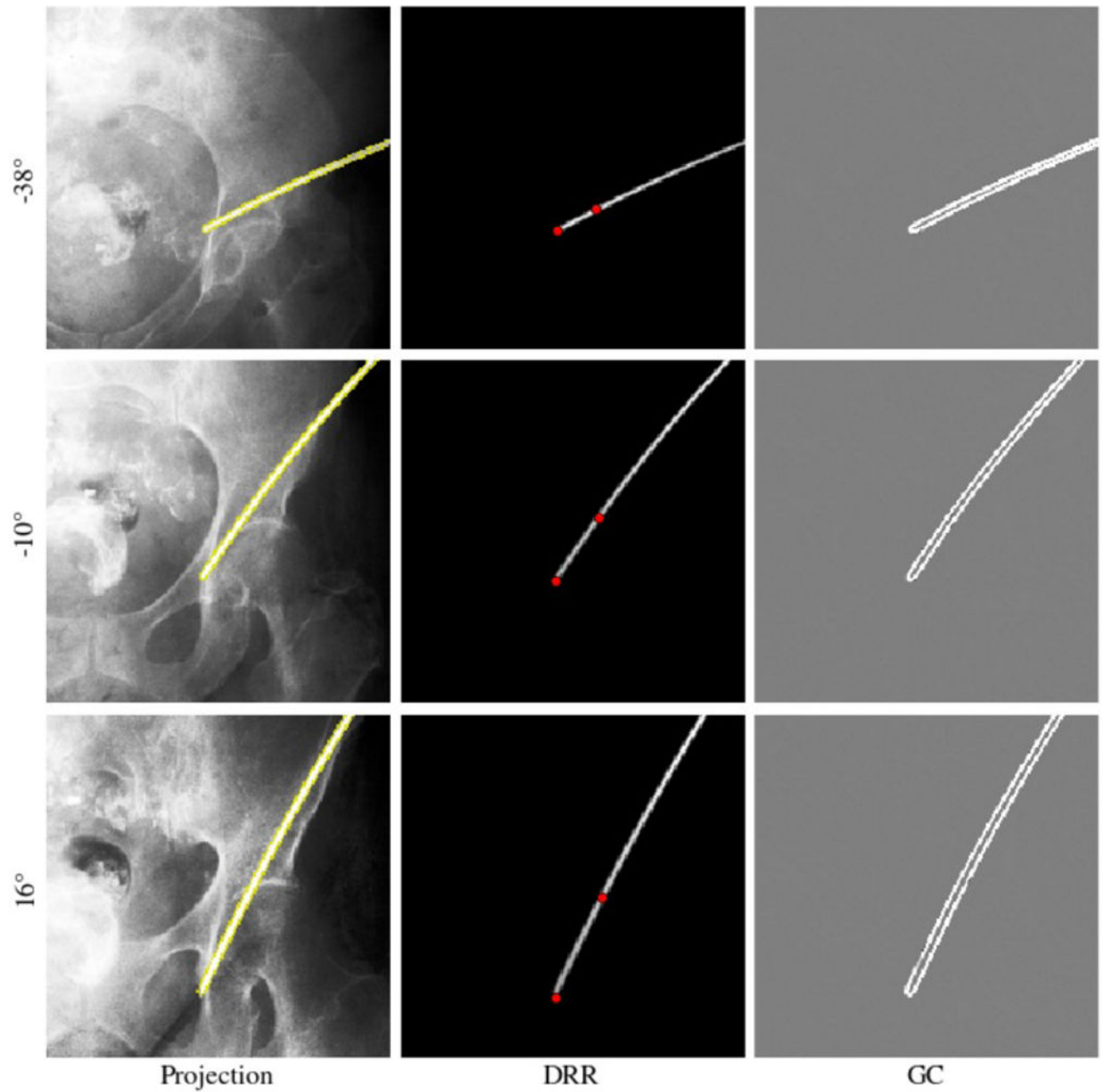


Figure 4.

Overview of the used projections (left column), DRRs (center column), and similarity metric GC (right column). The left column shows Known-component projections overlaid on (top) inlet view, (center) anterior posterior view, (bottom) outlet view. In the DRR column, manual annotation of the reference is projected and visualized by two red dots.